Cancer Research

ARN-509: A Novel Antiandrogen for Prostate Cancer Treatment

Nicola J. Clegg, John Wongvipat, James D. Joseph, et al.

Cancer Res 2012;72:1494-1503. Published OnlineFirst January 20, 2012.

Published OnlineFirst January 20, 2012; DOI:10.1158/0008-5472.CAN-11-3948

Therapeutics, Targets, and Chemical Biology

Cancer Research

ARN-509: A Novel Antiandrogen for Prostate Cancer Treatment

Nicola J. Clegg[1], John Wongvipat[1,2], James D. Joseph[10], Chris Tran[1], Samedy Ouk[9], Anna Dilhas[3], Yu Chen[1,8], Kate Grillot[10], Eric D. Bischoff[10], Ling Cai[1], Anna Aparicio[10], Steven Dorow[10], Vivek Arora[1,8], Gang Shao[10], Jing Qian[10], Hong Zhao[3], Guangbin Yang[3], Chunyan Cao[3], John Sensintaffar[10], Teresa Wasielewska[1], Mark R. Herbert[10], Celine Bonnefous[10], Beatrice Darimont[10], Howard I. Scher[8], Peter Smith-Jones[4], Mark Klang[5], Nicholas D. Smith[10], Elisa De Stanchina[6], Nian Wu[7], Ouathek Ouerfelli[3], Peter J. Rix[10], Richard A. Heyman[10], Michael E. Jung[9], Charles L. Sawyers[1,2], and Jeffrey H. Hager[10]

Abstract

Continued reliance on the androgen receptor (AR) is now understood as a core mechanism in castration-resistant prostate cancer (CRPC), the most advanced form of this disease. While established and novel AR pathway–targeting agents display clinical efficacy in metastatic CRPC, dose-limiting side effects remain problematic for all current agents. In this study, we report the discovery and development of ARN-509, a competitive AR inhibitor that is fully antagonistic to AR overexpression, a common and important feature of CRPC. ARN-509 was optimized for inhibition of AR transcriptional activity and prostate cancer cell proliferation, pharmacokinetics, and *in vivo* efficacy. In contrast to bicalutamide, ARN-509 lacked significant agonist activity in preclinical models of CRPC. Moreover, ARN-509 lacked inducing activity for AR nuclear localization or DNA binding. In a clinically valid murine xenograft model of human CRPC, ARN-509 showed greater efficacy than MDV3100. Maximal therapeutic response in this model was achieved at 30 mg/kg/d of ARN-509, whereas the same response required 100 mg/kg/d of MDV3100 and higher steady-state plasma concentrations. Thus, ARN-509 exhibits characteristics predicting a higher therapeutic index with a greater potential to reach maximally efficacious doses in man than current AR antagonists. Our findings offer preclinical proof of principle for ARN-509 as a promising therapeutic in both castration-sensitive and castration-resistant forms of prostate cancer. *Cancer Res; 72(6); 1494–503. ©2012 AACR.*

Introduction

Castration-resistant prostate cancer (CRPC) is the second most common cause of cancer-related deaths in American men (32,000 deaths/y; ref. 1). Treatment of localized tumors is often curative; however, metastatic disease emerges in approximately 25% of patients (2). The disease is initially sensitive to androgen deprivation therapies (castration-sensitive disease state), but resistance is inevitably acquired, leading to CRPC which is incurable. Despite administration of androgen-depleting therapies, continued androgen receptor (AR) signaling is a common feature of CRPC, attributed to AR gene amplification, AR gene mutation, increased AR expression, or increased androgen biosynthesis in prostate tumors (2). Bicalutamide, a clinically used antiandrogen, competes with androgens for binding AR; however, in the setting of CRPC, bicalutamide undergoes an antagonist-to-agonist switch, stimulating AR activity [measured by increased prostate-specific antigen (PSA), an AR-regulated target gene product] and prostate tumor cell growth. The continued reliance of CRPC on AR signaling offers opportunities to develop next generation antihormonal agents to treat this disease.

Recently, 2 agents targeting the androgen signaling axis have undergone late-stage clinical testing for treatment of men with CRPC (3). Abiraterone acetate targets 7-α-hydroxylase/17,20-lyase (CYP17A), thereby inhibiting residual androgen biosynthesis (4, 5), whereas MDV3100 is an antiandrogen discovered by the Sawyers/Jung groups in a screen for potent antiandrogens lacking agonist activity in context of AR overexpression (6, 7). In a phase III study, abiraterone acetate (plus the corticosteroid, prednisone) increased overall survival by 3.9

Authors' Affiliations: [1]Human Oncology & Pathogenesis Program, [2]Howard Hughes Medical Institute, [3]Organic Synthesis Core Facility, [4]Molecular Pharmacology & Chemistry, [5]Research Pharmacy Core Facility, [6]Antitumor Assessment Core Facility, [7]Analytical Pharmacology Core Facility, [8]Genitourinary Oncology Service, Department of Medicine, Memorial Sloan-Kettering Cancer Center, New York, New York; [9]Department of Chemistry and Biochemistry, University of California, Los Angeles, California; and [10]Aragon Pharmaceuticals, Inc., San Diego, California

Note: Supplementary data for this article are available at Cancer Research Online (http://cancerres.aacrjournals.org/).

Current address for S. Dorow: Caymen Chemical Company, Ann Arbor, Michigan.

Corresponding Authors: Charles L. Sawyers, Human Oncology & Pathogenesis Program, Howard Hughes Medical Institute, Memorial Sloan-Kettering Cancer Center, 1275 York Avenue Box 20, New York, NY 10065. Phone: 646-888-2594; Fax: 646-888-2595; E-mail: sawyersc@mskcc.org; and Jeffrey H. Hager, Aragon Pharmaceuticals, Inc., 12780 El Camino Real, Suite 301, San Diego, CA 92130. Phone: 858-369-7608; Fax: 858-369-7656; E-mail: jhager@aragonpharm.com

doi: 10.1158/0008-5472.CAN-11-3948

Published OnlineFirst January 20, 2012; DOI:10.1158/0008-5472.CAN-11-3948

months over control (prednisone only) in patients with CRPC previously treated with docetaxel (8). Coadministration of low-dose prednisone is necessary to ameliorate hypertension, hypokalemia, and fluid overload resulting from mineralocorticoid excess induced by CYP17 inhibition (8). Whereas coadministration of prednisone is manageable in patients with metastatic CRPC, longer term use in earlier disease phases could be problematic due to potential side effects (diabetes, weight gain, Cushing syndrome, and osteoporosis). In phase I/II studies of MDV3100, significant serum–PSA responses (>50% decrease) were observed in more than 50% of patients with chemotherapy-naive and -treated CRPC. MDV3100 belongs to a class of antiandrogens that carry seizure risk, likely mediated via antagonism of the central nervous system (CNS)-based $GABA_A$ receptor (9). MDV3100 dosing regimens must achieve exposures at steady state sufficient to drive therapeutic response without exceeding the threshold for adverse effects. Antiandrogens with a high therapeutic index can be expected to result in safer, more effective treatments across all stages of prostate cancer.

We describe the discovery and preclinical development of ARN-509, an antiandrogen with similar *in vitro* activity to MDV3100 but with greater *in vivo* activity in CRPC xenograft models (6). ARN-509 exhibits antitumor activity in a castration-sensitive xenograft model of prostate cancer and antiandrogenic effects in dogs that phenocopy castration. ARN-509, like MDV3100 and other antiandrogens, binds weakly to $GABA_A$ receptors and could potentially cause seizure at high dose. However, mouse steady-state plasma and brain levels are lower for ARN-509 versus MDV3100 at therapeutic doses, suggesting lower seizure-inducing potential for ARN-509. These data support clinical development of ARN-509 for treatment of castration-sensitive and -resistant prostate cancer.

Materials and Methods

Detailed information is presented in Supplementary Materials and Methods. Ligand-binding studies were conducted either in a whole-cell assay [LNCaP/AR(cs)], using whole-cell extracts (MDA-MB-453), or *in vitro* with purified receptor. Proliferation assays (VCaP) were conducted in either agonist or antagonist mode (without/with R1881). RNA was isolated from LNCaP/AR cells for quantitative RT-PCR analysis with primers (Supplementary Table S1) specific for AR target genes. Fluorescence microscopy was carried out in LNCaP cells transfected with AR tagged with enhanced yellow fluorescent protein (AR-EYFP) as previously described (6). AR antibody PG-21 (Upstate) was used for chromatin immunoprecipitation (ChIP) experiments [LNCaP/AR(cs)] together with primers for PSA (10) and TMPRSS2 (11) enhancers. Luciferase reporter gene assays were conducted in LNCaP/AR-luc or Hep-G2 cells expressing VP16-AR.

Animal studies at Memorial Sloan-Kettering Cancer Center (MSKCC, New York), Aragon Pharmaceuticals, and Covance Laboratories, Inc. were conducted under protocols approved by MSKCC or Aragon Institutional Animal Care and Use Committees and institutional guidelines for humane use of animals in research were followed. *In vivo* xenograft experiments [LNCaP/AR(cs) or LNCaP/AR-luc] and terminal deoxynucleotidyl transferase–mediated dUTP nick end labeling (TUNEL) and Ki-67 staining were carried out as previously described (6). As part of an Investigational New Drug (IND) enabling toxicity/toxicokinetic study, ARN-509 was administered to male beagle dogs by Covance Laboratories, Inc., in accordance with U.S. Food and Drug Administration (FDA) Good Laboratory Practice (GLP) Regulations. Histologic image files are available online (12). Mouse/dog pharmacokinetics was determined by noncompartmental analysis. Tumor and brain tissue distribution was quantified by liquid chromatography/tandem mass spectrometry (LC-MS/MS). Serum–protein binding was assessed *in vitro* by equilibrium dialysis, using mouse and human plasma. $GABA_A$-binding experiments in membrane homogenates of rat cerebral cortex used [^{35}S]TBPS competitor with picrotoxin as a positive-control.

Results

ARN-509 binds AR and inhibits growth and androgen-mediated gene transcription in AR-overexpressing prostate cancer cells

ARN-509 (Fig. 1A) is a synthetic biaryl thiohydantoin compound discovered using structure–activity relationship (SAR)-guided medicinal chemistry to identify nonsteroidal antiandrogens that retain full antagonist activity in the setting of increased AR expression.

Equilibrium-binding affinity of ARN-509 for AR was measured in competition with 16β-[^{18}F]fluoro-5α-DHT (^{18}F-FDHT) in a whole-cell binding assay [LNCaP/AR(cs) cells; Fig. 1B). ARN-509 (IC_{50} = 16 nmol/L) binds AR with 7- to 10-fold greater affinity than the clinically approved antiandrogen, bicalutamide (median IC_{50} = 160 nmol/L) and competes for the same binding site in the ligand-binding pocket of the receptor. Curiously, AR-binding assays using MDA-MB-453 cell extracts does not differentiate between ARN-509 and bicalutamide, possibly due to cellular uptake differences in the whole-cell binding assay (Supplementary Fig. S1). Binding of ARN-509 is selective for AR versus other nuclear hormone receptors (up to 100 μmol/L), as shown in competitive-binding assays using *in vitro* purified AR or estrogen, progesterone, or glucocorticoid receptors (ER, PR, or GR; Supplementary Table S2).

Identification of ARN-509 as a lead candidate for preclinical development was based on initial assessment of both antagonist and agonist activity of AR signaling in the LNCaP/AR(cs) prostate cancer cell line. This cell line was engineered to overexpress AR (3- to 5-fold higher than parental LNCaP), thus mimicking the castration-resistant clinical state (2, 13). In castration-resistant LNCaP/AR cells, ARN-509 (and MDV3100) antagonized androgen-mediated induction or repression of mRNA expression levels for 13 endogenous genes including PSA and TMPRSS2 whereas bicalutamide was significantly less effective (Fig. 1C). Bicalutamide treatment of LNCaP/AR(cs) cells in absence of the synthetic androgen R1881 resulted in altered gene expression consistent with its well-documented agonist activity in context of AR overexpression. ARN-509 or

Published OnlineFirst January 20, 2012; DOI:10.1158/0008-5472.CAN-11-3948

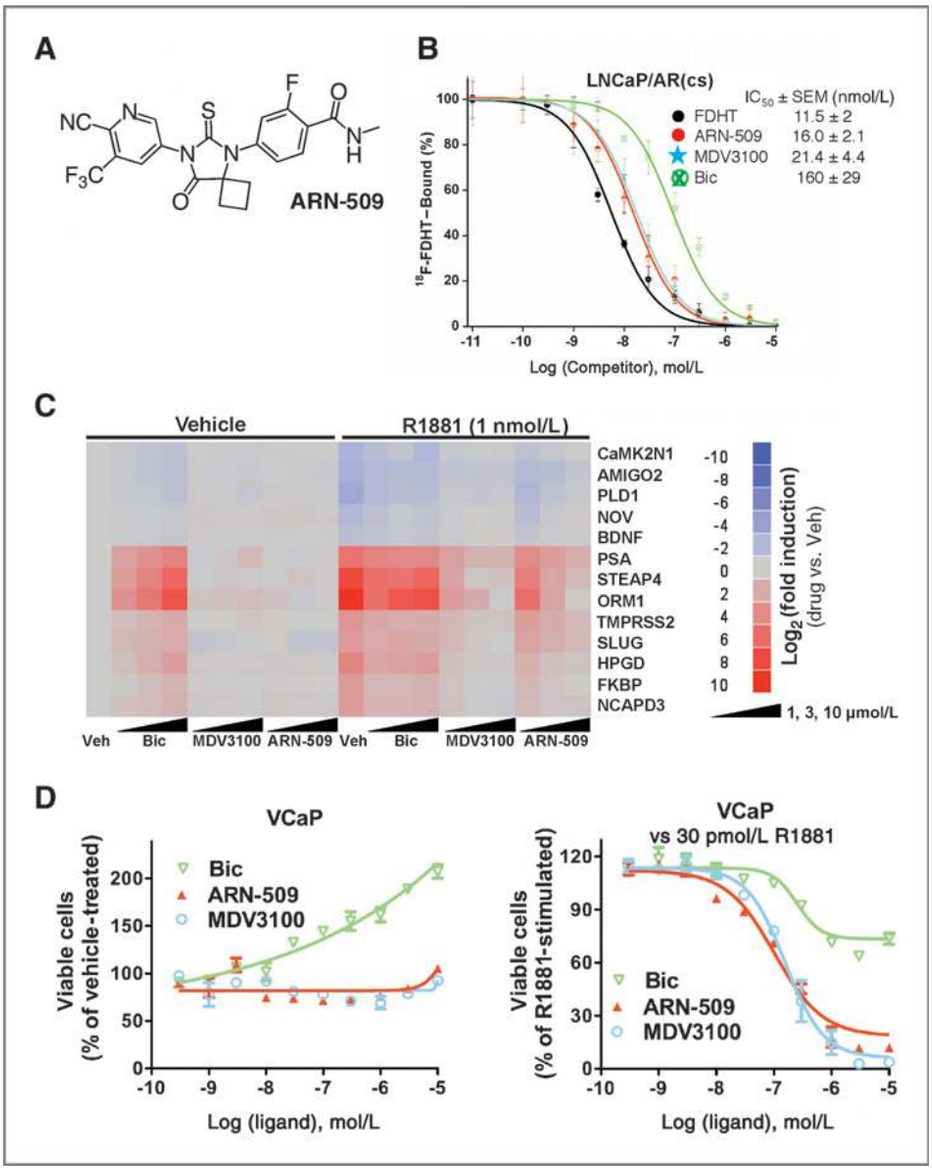

Figure 1. ARN-509 activity *in vitro* in human prostate cancer cells. A, ARN-509 structure. B, representative competitive-binding assay versus ^{18}F-FDHT [LNCaP/AR(cs)]. IC_{50} values: 11.5 nmol/L (FDHT), 16 nmol/L (ARN-509), 21.4 nmol/L (MDV3100), 160 nmol/L. Bic, bicalutamide. Error bars, SD; $n = 3$. Inset, IC_{50} values (mean ± SEM) from 5 replicate experiments. C, qRT-PCR analysis of AR-regulated genes [(normalized to glyceraldehyde-3-phosphate dehydrogenase (GAPDH)]. LNCaP/AR(cs) cultured (5% CSS) 3 days with or without 1 nmol/L R1881 and DMSO (Veh) or drug (1, 3, and 10 μmol/L). D, VCaP cultured (5% CSS) for 2 days, then treated for 7 days. Left, agonist mode. Right, antagonist mode with 30 pmol/L R1881. Viable cells (CellTiter-Glo) plotted as percentage of vehicle control (DMSO; $n = 3$, mean ± SEM).

MDV3100 did not exhibit agonist activity up to 10 μmol/L (Fig. 1C). Similar results were obtained with a second, independently derived LNCaP/AR line harboring a stably integrated AR-regulated probasin:luciferase reporter construct (ARR2-Pb-luc; Fig. 2C).

To determine whether inhibition of AR signaling by ARN-509 is accompanied by reduced tumor cell proliferation, the number of viable prostate cancer cells was quantified following incubation with antiandrogen. ARN-509 fails to stimulate proliferation of VCaP cells (Fig. 1D, left) and antagonized the proliferative effect of R1881 (Fig. 1D, right), whereas bicalutamide induced cell proliferation in a dose-dependent manner (Fig. 1D, left), and only partially antagonized the effects of R1881 (Fig. 1D, right). There was no significant effect on growth of AR-negative PC-3 prostate cancer cells, indicating that antiproliferative effect observed in VCaP cells is mediated through antagonism of AR (Supplementary Fig. S2).

ARN-509 impairs nuclear localization and DNA binding in prostate cancer cells

Translocation of AR from cytoplasm to nucleus upon ligand binding is a highly regulated essential step in AR-mediated gene regulation. To determine whether ARN-509 impairs AR nuclear localization and thus reduces the concentration of AR available to bind androgen response elements (ARE), LNCaP cells expressing AR-EYFP were treated with dimethyl sulfoxide (DMSO), R1881, bicalutamide, or ARN-509. Fluorescence intensities of nuclear (N) and cytoplasmic (C) compartments of individual cells were quantified and the N/C ratio calculated. In DMSO-treated cells, AR-EYFP was largely localized to the cytoplasm (N/C ratio, 0.7), whereas in R1881-treated cells the

Published OnlineFirst January 20, 2012; DOI:10.1158/0008-5472.CAN-11-3948

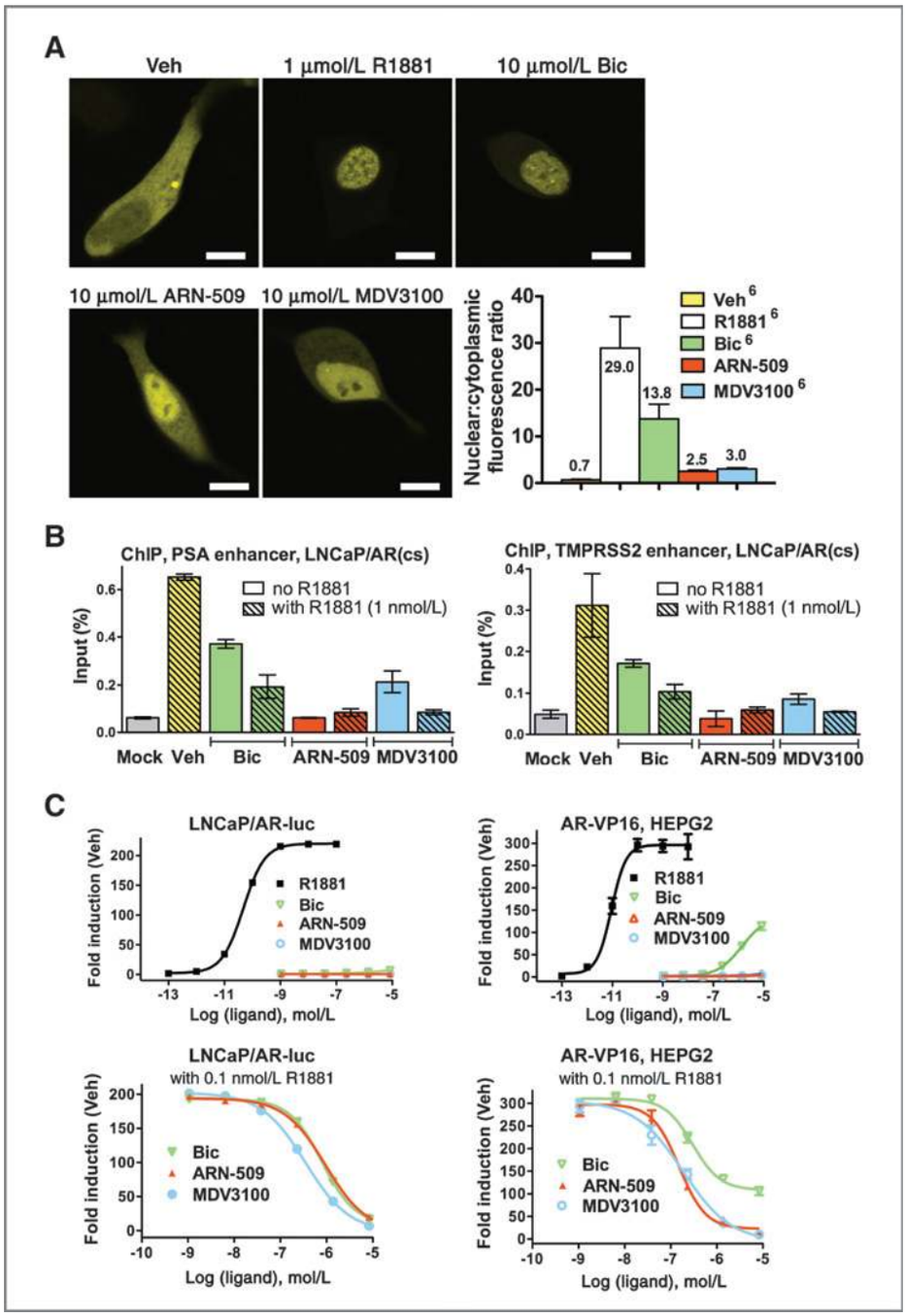

Figure 2. ARN-509 impairs AR nuclear localization and inhibits DNA binding. A, representative confocal microscopic images (scale bars, 10 μm) of LNCaP with AR-EYFP cultured (5% CSS) and treated with DMSO (Veh) or drug. Nuclear: cytoplasmic fluorescence intensity of individual cells was quantified ($n = 3$, mean $\pm$ SEM). B, ChIP of AR in LNCaP/AR(cs) cultured (5% CSS) and treated 1 hour with or without 1 nmol/L R1881 and either DMSO (Veh) or 10 μmol/L antiandrogen. RT-PCR: PSA, TMPRSS2 enhancers (mean $\pm$ SD, $n = 2$). C, activation of an androgen-regulated 4XARE-luc reporter gene by wild-type AR and VP16-AR in LNCaP/AR-luc or Hep-G2 cells treated for 40 to 48 hours with or without 0.1 nmol/L R1881 and either DMSO (Veh) or antiandrogen. Luciferase assay conducted on cell lysates: light units relative to vehicle control ($n = 3$, mean $\pm$ SEM).

receptor was localized predominantly in the nucleus (N/C ratio, 29; Fig. 2A). Bicalutamide treatment also resulted in a significant amount of nuclear AR (N/C ratio, 13.8), although less than that observed with R1881 (ref. 6; Fig. 2A). In contrast, in ARN-509–treated cells much of the AR-EYFP protein remained cytoplasmic (N/C ratio, 2.5; Fig. 2A). This decrease in nuclear AR was unrelated to turnover or stability, as ARN-509 did not alter steady-state levels of AR as monitored by immunoblot of whole-cell lysates (data not shown).

To explore whether the low levels of nuclear AR following ARN-509 treatment could be recruited to promoters of target genes in prostate cancer cells with potential to modulate transcription, we carried out ChIP experiments in LNCaP/AR cells treated with R1881 and/or antiandrogen. AR was not recruited to the enhancer region of PSA or TMPRSS2 target genes after ARN-509 or MDV3100 treatment under hormone-depleted conditions (Fig. 2B). In antagonist mode (cotreatment with R1881 to activate AR), ARN-509 was able to effectively

Published OnlineFirst January 20, 2012; DOI:10.1158/0008-5472.CAN-11-3948

compete with R1881 and prevent AR from binding to promoter regions (Fig. 2B). In contrast, bicalutamide exhibited partial agonist activity as evidenced by induction of DNA binding at AR target genes and incomplete antagonism of the effects of R1881 (Fig. 2B).

AR recruitment to DNA promoter elements and activation of gene transcription requires interplay of protein cofactors in response to receptor conformational changes upon ligand binding (14). To remove cofactor recruitment as a variable that might explain the effects of ARN-509 on AR DNA binding, we directly assessed the DNA-binding competency of the residual nuclear AR in ARN-509–treated Hep-G2 cells expressing a VP16-AR fusion protein and an ARE-driven luciferase reporter. VP16-AR is constitutively nuclear and drives transcription through AREs in the absence of coactivator protein recruitment, thereby providing a direct assessment of ligand-induced DNA binding (6, 14). In absence of R1881, bicalutamide partially activated VP16-AR–mediated

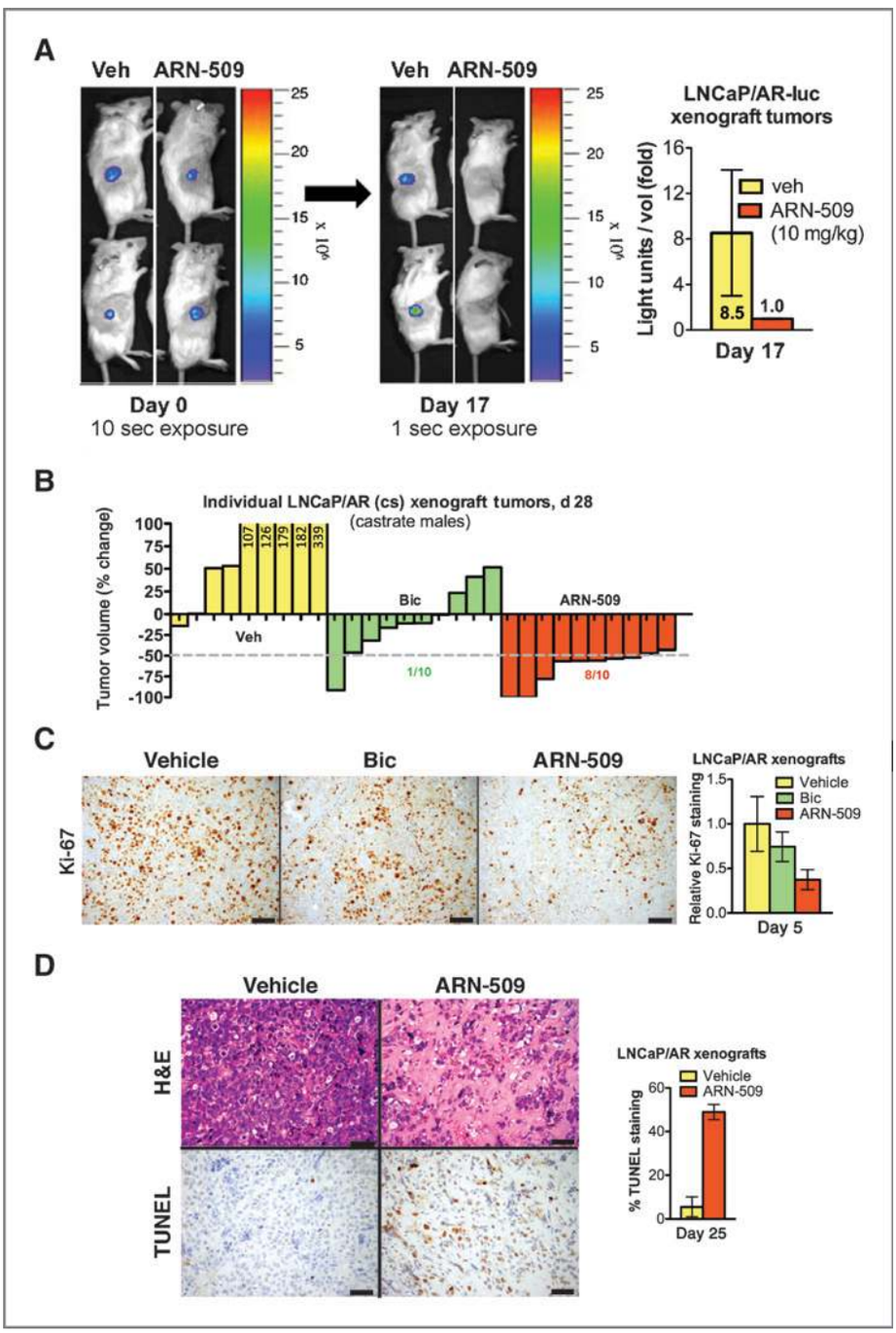

Figure 3. ARN-509 is active in models of CRPC. A, luciferase imaging of castrate male mice harboring LNCaP/AR-luc tumors pretreatment (day 0) and posttreatment (day 17), normalized to tumor volume. B, castrate male mice bearing LNCaP/AR(cs) tumors (mean tumor volume, 200 mm^3) treated by daily gavage with vehicle or drug (10 mg/kg/day). Percentage of change in individual tumor volume (9–10 tumors per treatment group) after 28 days. Unpaired *t* test: vehicle versus ARN-509, $P = 0.0001$; vehicle versus Bic, $P = 0.004$; ARN-509 versus Bic, $P = 0.002$. Plasma concentrations measured 24 hours postdose on day 28 (mean ± SEM: Bic, 30.74 ± 3.68; ARN-509, 9.69 ± 1.58). C, castrate male mice bearing LNCaP/AR tumors more than 100 mm^3 treated 5 days by daily gavage with vehicle or 10 mg/kg/d antiandrogen. Ki-67 immunohistochemistry carried out on tumor tissue resected 2 hours after final dose. Number positively stained cells calculated out of 300 cells counted in each of 5 random views ($n = 3$ tumors per treatment group) and expressed relative to vehicle controls [error, SD; Veh vs. ARN-509 and Bic vs. ARN-509, $P > 0.05$ (1-way ANOVA with the Bonferroni posttest)]. D, castrate male mice bearing LNCaP/AR tumors treated as in (C) for 25 days. TUNEL staining carried out on tumor tissue resected after final dose. Number positively stained cells calculated out of 300 cells counted in each of 5 random views ($n = 3$ tumors per treatment group), expressed relative to vehicle controls (error, SD).

Published OnlineFirst January 20, 2012; DOI:10.1158/0008-5472.CAN-11-3948

transcription, indicative of AR binding to DNA. In LNCaP/AR-luc cells with a stably integrated AR-driven luciferase reporter construct (6, 14), bicalutamide was unable to activate wild-type AR (Fig. 2C, top left). In contrast to bicalutamide, ARN-509 did not induce significant VP16-AR–mediated transcription and thus is not competent to induce significant DNA binding at concentrations up to 10 μmol/L (Fig. 2C, top right). ARN-509 and MDV3100 inhibited R1881-induced VP16-AR–mediated transcription with an IC_{50} value of 0.2 μmol/L (Fig. 2C). In contrast, in the presence of R1881, bicalutamide showed only weak partial antagonism of VP16-AR–mediated transcription ($IC_{50} = 0.35$ μmol/L; Fig. 2C, bottom right). This confirms the ChIP findings and underscores the fundamental mechanistic differences between ARN-509 versus bicalutamide.

ARN-509 is a potent inhibitor of tumor growth in murine xenograft models of CRPC

ARN-509 exhibits low systemic clearance, high oral bioavailability, and long plasma half-life in both mouse and dog, supporting once daily oral dosing (Supplementary Table S3). Consistent with its long terminal half-life, ARN-509 steady-state plasma levels increased in repeat dose studies, resulting in high C_{24h} levels and low peak:trough ratios (ratio, 2.5; Supplementary Table S4). To assess *in vivo* pharmacodynamic activity of ARN-509 in a model of CRPC, castrate male immunodeficient mice harboring LNCaP/AR-luc xenograft tumors (coexpressing exogenous AR and the AR-dependent reporter ARR2-Pb-luc) were orally treated with either vehicle or ARN-509 (10 mg/kg/d). Following 17 days of treatment, androgen-driven luciferase reporter–gene activity, normalized to tumor volume, was consistently reduced in ARN-509–treated animals compared with vehicle (Fig. 3A), indicating AR inhibition by ARN-509 *in vivo*.

The therapeutic effect of ARN-509 (10 mg/kg/d) was compared with bicalutamide (10 mg/kg/d) in castrate mice bearing LNCaP/AR(cs) xenograft tumors. On day 28, 7 of 9 vehicle-treated tumors increased in size compared with starting volume (Fig. 3B, yellow). The antitumor activity of bicalutamide in this model was largely restricted to growth inhibition rather than tumor shrinkage––only 1 of 10 tumors exhibited more than 50% regression (Fig. 3B, green). In contrast, 8 of 10 ARN-509–treated tumors regressed by more than 50% (volume), including 2 tumors that were no longer palpable (Fig. 3B, red). Similar results were obtained in castrate male SCID mice bearing LNCaP/AR-luc xenograft tumors (Supplementary Fig. S3). Greater efficacy of ARN-509 was achieved despite 3-fold lower steady-state plasma levels (mean C_{24h} concentrations: 9.69 μg/mL ARN-509 vs. 30.74 μg/mL bicalutamide). Consistent with the potent antitumor effect, ARN-509–treated tumors exhibited a 60% decrease in proliferative index (vs. vehicle) and a 10-fold increase in apoptotic rate (vs. vehicle) as monitored by Ki-67 staining and TUNEL, respectively (Fig. 3C and D).

To further understand the clinical potential of ARN-509, we compared its antitumor activity to MDV3100 in a series of independent experiments. Castrate male mice bearing LNCaP/AR xenograft tumors were treated with either ARN-509 or MDV3100 at doses of 1, 10, or 30 mg/kg/d. Both compounds showed a dose-responsive effect (Fig. 4A and B)

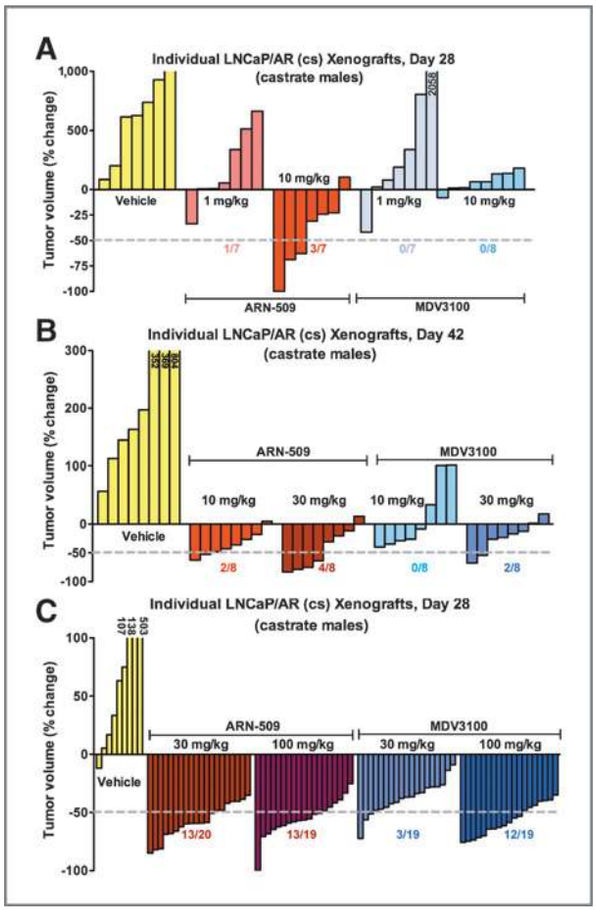

Figure 4. ARN-509 achieves similar efficacy with lower steady-state plasma levels than MDV3100 in LNCaP/AR xenograft models of CRPC. A–C, castrate male mice bearing LNCaP/AR(cs) tumors treated by oral daily gavage with vehicle, ARN-509, or MDV3100. Unpaired *t* test used for statistical comparisons. A, one and 10 mg/kg dose: percentage of change in individual tumor volume ($n = 7$–8 per treatment group) after 28-day treatment. $P < 0.05$, drug versus vehicle. B, ten and 30 mg/kg dose: percentage of change in individual tumor volume ($n = 8$ per treatment group) after 42-day treatment. $P < 0.05$, drug versus vehicle. C, thirty and 100 mg/kg dose: percentage of change in individual tumor volume ($n = 19$–20 tumors per treatment group) after 28-day treatment. $P < 0.05$, drug versus vehicle or ARN-509 30 mg/kg/day versus MDV3100 30 mg/kg/day.

trending towards greater efficacy for ARN-509 versus MDV3100, although none of the pairwise (equidose) comparisons of day 28 tumor volumes reached statistical significance, due to relatively small cohort size ($n = 7$–8). To define the optimal biological dose (OBD: lowest dose yielding maximum efficacy) for both ARN-509 and MDV3100, tumor responses in the LNCaP/AR(cs) model were monitored at 30 and 100 mg/kg/d in larger cohorts to increase statistical power ($n = 19$–20). Thirteen of 20 ARN-509 (30 mg/kg/d)-treated animals exhibited more than 50% reduction in tumor volume at day 28 versus 3 of 19 MDV3100 (30 mg/kg/d)-treated mice (Fig. 4C). A higher MDV3100 dose (100 mg/kg/d) resulted in increased efficacy (12 of 19 tumors with >50% reduction in tumor volume) compared with the

Published OnlineFirst January 20, 2012; DOI:10.1158/0008-5472.CAN-11-3948

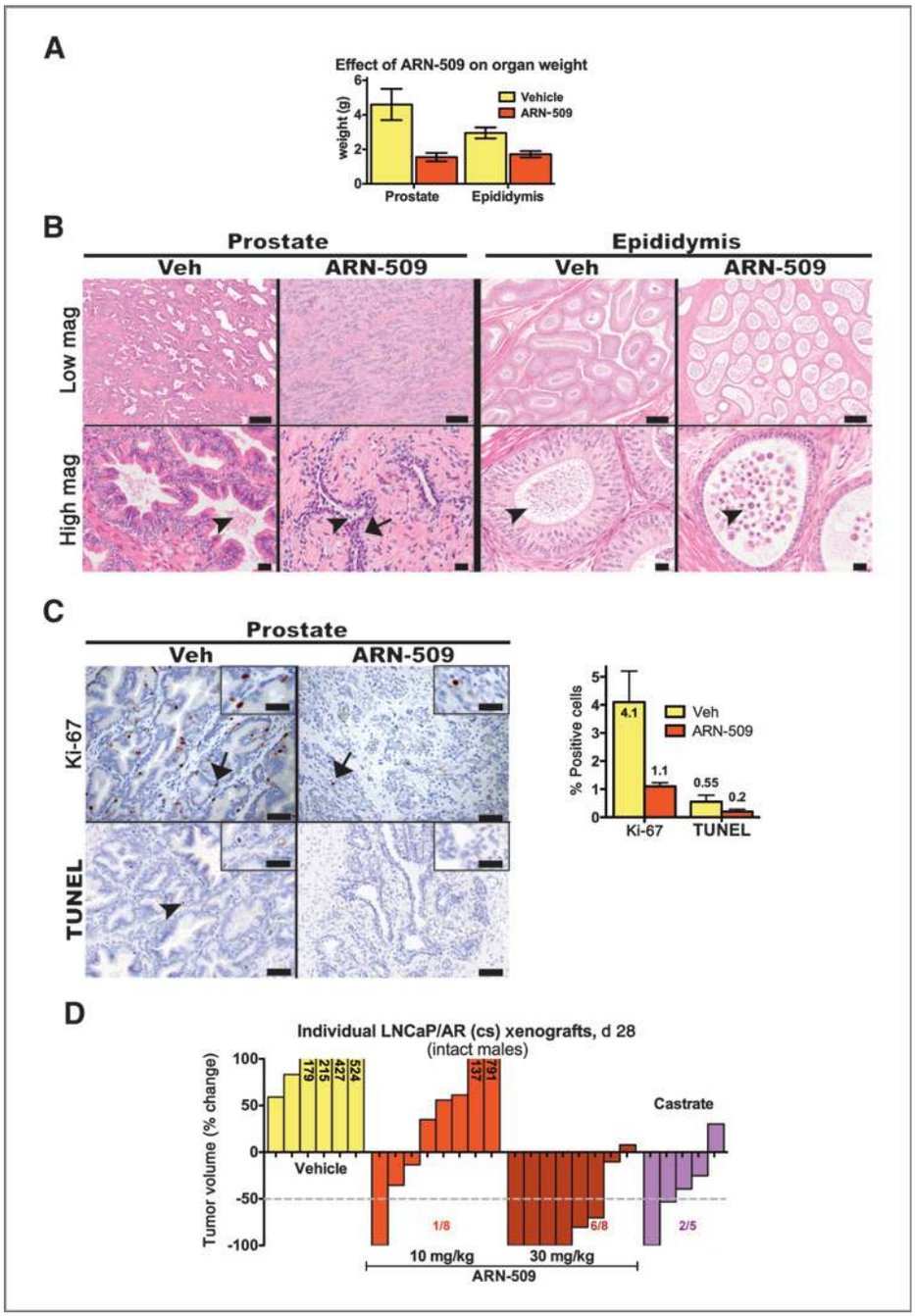

Figure 5. ARN-509 induces castrate-like changes in dog prostate and epididymis. A–C, intact male beagle dogs treated by oral gavage for 28 days with vehicle ($n = 5$) or ARN-509 10 mg/kg/d ($n = 4$). Organs resected 24 hours after final dose. Mean plasma concentration of ARN-509 measured at sacrifice, 24 hours after final dose, was 17.5 μg/mL. A, prostate and epididymis weights (mean ± SEM). $P < 0.05$, Veh versus ARN-509 in prostate (2-way ANOVA, with the Bonferroni posttest). Comparison for epididymis is insignificant. B, hematoxylin and eosin (H&E) staining of transverse prostate sections (top) and longitudinal epididymis sections (bottom) at low power (100 ×; scale bar, 200 μm) and high power (600 ×; scale bar, 20 μm). Top, fully mature, active acini in vehicle-treated prostate containing intraluminal secretions (arrowhead), lined with folds of a single layer of columnar epithelial cells with abundant cytoplasm. ARN-509–treated prostates: bilayer of cuboidal epithelial cells (arrow), small lumens with rare eosinophilic secretory material (arrowhead). Bottom, vehicle-treated epididymis: tall columnar pseudostratified epithelium with lumens containing abundant spermatozoa (arrowhead). ARN-509–treated epididymis: cuboidal epithelium, lumens with little-to-no spermatozoa, containing multinucleated round cells suggestive of sloughed degenerate germ cells (arrowhead). C, dog prostates stained with antibody to Ki-67 (200 ×; scale bar, 100 μm) or TUNEL (400 ×; scale bar, 50 μm). Ki-67 staining (arrows) and TUNEL (arrowheads). No TUNEL staining is evident in ARN-509–treated prostates. Results quantified as mean percentage (± SEM) of positive cells from representative areas from each prostate ($n = 5$ for vehicle, $n = 4$ for ARN-509). $P < 0.05$ for TUNEL staining of Veh versus ARN-509 (1-way ANOVA with the Bonferroni multiple comparison posttest). D, intact male mice bearing LNCaP/AR(cs) tumors, treated for 28 days by oral daily gavage with vehicle, ARN-509, or MDV3100 (10 and 30 mg/kg). Percentage of change in individual tumor volume ($n = 5$–8 per treatment group) after 28-day treatment. $P < 0.05$ for each treatment relative to vehicle (unpaired t test).

Published OnlineFirst January 20, 2012; DOI:10.1158/0008-5472.CAN-11-3948

Table 1. ARN-509 and MDV3100 steady-state levels in plasma and in LNCaP/AR(cs) xenograft tumor tissue after 28-day dosing

Dose, mg/kg/d	# mice	Plasma C_{24h}, μg/mL[a]	Tumor C_{24h}, μg/g[a]	Tumor:plasma ratio (%)
ARN-509				
1	6	0.425 ± 0.16	0.991 ± 0.30	259 ± 11
10	5	3.31 ± 0.98	3.26 ± 0.82	107 ± 44
MDV3100				
1	5	1.08 ± 0.26	0.439 ± 0.12	45.1 ± 24.8
10	7	11.0 ± 2.5	3.39 ± 1.50	30.5 ± 12.8

NOTE: After 28 days of dosing at 1 and 10 mg/kg/d, plasma and tumor–tissue concentrations of ARN-509 and MDV3100 were quantified 24 hours after final drug dose with an LC/MS/MS method.
[a]mean ± SD.

30 mg/kg/d dose. In contrast, ARN-509 dosed at 100 mg/kg/d (13 of 19 mice with >50% reduction in tumor volume) was no more efficacious than 30 mg/kg/d. There was no difference in efficacy between ARN-509 and MDV3100 at 100 mg/kg/d, despite a dose-dependent increase in exposure (ARN-509 and MDV3100 from 30–100 mg/kg) as measured by independent single-dose mouse pharmacokinetic studies (Supplementary Table S5). These results indicate an OBD in the LNCaP/AR model between 10 to 30 mg/kg/d for ARN-509, whereas the OBD for MDV3100 lies between 30 to 100 mg/kg/d.

To define concentrations of ARN-509 necessary to drive therapeutic responses, we measured steady-state plasma and tumor–tissue concentrations following 28 days of continuous dosing of LNCaP/AR(cs) tumor-bearing mice. Steady-state plasma concentrations for ARN-509 were approximately 2- to 4-fold lower than for an equivalent dose of MDV3100 (Table 1 and Supplementary Table S5), whereas intratumoral levels of ARN-509 and MDV3100 were roughly equivalent, indicating a higher tumor/plasma ratio for ARN-509 (Table 1). A comparative single-dose intravenous pharmacokinetic assessment in mice indicated higher steady-state volume-of-distribution (V_{ss}) for ARN-509 (2.1 L/kg; Supplementary Table S3) versus MDV3100 (0.82 L/kg; Supplementary Table S6). One determinant of V_{ss} is degree of binding to plasma proteins. Assessment of *in vitro* free fraction in plasma indicated that ARN-509 is less protein bound, resulting in an approximately 2-fold greater free fraction than MDV3100 in mouse and human plasma (Supplementary Table S7).

Recent reports indicate that multiple antiandrogens are also functional antagonists of the $GABA_A$ receptor, implicated to cause seizure in preclinical species and in humans (9). ARN-509 and MDV3100 both exhibit low micromolar affinity ($IC_{50} = 3.0$ and 2.7 μmol/L, respectively) for the $GABA_A$ receptor in radioligand binding assays (Supplementary Fig. S4) and thus may potentially antagonize $GABA_A$ at therapeutic dose levels. Degree of permeability of the blood–brain barrier to ARN-509 or MDV3100 is a further determinant of seizure risk. Steady-state brain tissue levels of both ARN-509 and MDV3100 (10 mg/kg/d) were measured in mice after 28 days of daily therapy. Unexpectedly, ARN-509 brain levels were 4-fold lower than those observed with MDV3100 treatment (Table 2), thus suggesting lower seizurogenic potential for ARN-509.

ARN-509 induces castrate-like histopathologic changes in androgen-dependent tissues in dogs

Robust antiandrogenic activity in the noncastrate setting would support clinical assessment of ARN-509 in the castration-sensitive phase of prostate cancer. To determine antiandrogenic effects of ARN-509 in context of normal levels of androgen, we assessed effects on androgen-dependent reproductive organs of adult male dogs and on LNCaP/AR xenograft tumor growth in intact male mice.

Table 2. ARN-509 and MDV3100 steady-state levels in plasma and brain tissue

Dose, mg/kg/d	# mice	Plasma C_{24h}, μg/mL[a]	Brain C_{24h}, μg/g[a]	Brain:plasma (%)
ARN-509				
10	8	1.64 ± 0.30	0.479 ± 0.132	29.3 ± 6.3
MDV3100				
10	5	10.5 ± 2.3	2.01 ± 0.83	18.8 ± 4.4

NOTE: ARN-509 and MDV3100 were measured in plasma or brain tissue following 28-day daily dosing at 10 mg/kg/d. Plasma and brain were isolated 24 hours after final dose on day 28. ARN-509 and MDV3100 levels quantified with an LC/MS/MS method.
[a]mean ± SD.

Published OnlineFirst January 20, 2012; DOI:10.1158/0008-5472.CAN-11-3948

ARN-509 dosed at 10 mg/kg/d for 28 days resulted in a 3-fold reduction in weight of dog prostates. Epididymis weight was also reduced (1.7-fold); however, this effect did not reach statistical significance (Fig. 5A). Histopathologic analysis of prostates of ARN-509–treated animals showed lack of glandular secretory activity, similar to prostates of sexually immature or castrate animals (Fig. 5B, right).

Antiandrogenic effects on spermatogenesis were evident in ARN-509–treated animals. Epididymides of ARN-509–treated animals exhibited histologic changes consistent with antiandrogen-induced atrophy and contained minimal spermatozoa (Fig. 5B, left). Epididymides of vehicle-treated dogs were normal, with abundant spermatozoa (Fig. 5B, left).

Cell proliferation in dog prostate tissues treated with ARN-509 was significantly lower (reduced Ki-67 staining) than in vehicle-treated animals (Fig. 5C). Despite significant atrophy and the well-described increase in prostatic apoptosis following castration (15), there was no change in apoptotic rate in ARN-509–treated prostates (TUNEL staining), suggesting that atrophy, if driven by apoptosis, was advanced and complete at 28 days of treatment (Fig. 5C). The epididymides of ARN-509–treated animals exhibited a tendency towards lower proliferative and higher apoptotic indices compared with vehicle-treated animals, although Ki-67- or TUNEL-positive cells were rare (Supplementary Fig. S5).

Consistent with the antiandrogenic effects observed in the dog, ARN-509 displayed significant antitumor activity in LNCaP/AR(cs) xenografts growing in intact (noncastrate) mice (Fig. 5D). At 10 mg/kg/d, the antitumor effect of ARN-509 was largely confined to stabilization of tumor growth. At higher doses of 30 mg/kg/d, robust tumor regression (>50% reduction in starting tumor volume) was observed in 6 of 8 ARN-509–treated animals, similar to regressions observed in mice castrated on the day treatment initiated.

Discussion

ARN-509 is a next generation antiandrogen selected for preclinical and clinical development based on its efficacy and pharmacodynamic profile in mouse xenograft models of CRPC. Unexpectedly, given a similar *in vitro* profile, ARN-509 is more efficacious per unit dose and per unit steady-state plasma level in mouse models of CRPC than MDV3100. Maximal efficacy at lower steady-state plasma and brain levels should result in a higher therapeutic index and enable dose-escalation in man with reduced risk of seizure and other side effects. We propose that the ability of ARN-509 to drive efficacy with significantly lower exposures at steady state is a function of reduced binding to plasma proteins, resulting in greater tumor:plasma ratios and more robust antagonism of AR activity. Importantly and unexpectedly, the greater free fraction of ARN-509 does not result in higher steady-state brain levels which otherwise could negate any increase in therapeutic index as it relates to $GABA_A$ antagonism.

The ARN-509 pharmacologic effects on male reproductive organs, and antitumor activity on LNCaP/AR tumors in intact mice, suggests potential to treat the castration-sensitive disease phase. In particular, given the improved profile of ARN-509 over bicalutamide, "combined androgen blockade" [ARN-509 dosed in conjunction with luteinizing hormone–releasing hormone (LHRH) agonists/antagonists] may be useful in treatment of recurrent disease following primary treatment by surgery or radiation. Given its potential for a high therapeutic index, ARN-509 is also well suited to combination therapy with other agents that target key pathways [e.g., phosphoinositide 3-kinase (PI3K)] in prostate tumorigenesis (16).

ARN-509 has completed dose-escalation phase I study in metastatic CRPC to determine human pharmacokinetics, safety, and efficacy (via endpoints of PSA response and time-to-PSA progression) and has proceeded into phase II clinical development in distinct subsets of prostate cancer.

Disclosure of Potential Conflicts of Interest

J. Wongvipat, C. Tran, S. Ouk, M. Jung, and C.L. Sawyers are coinventors of ARN-509 and MDV3100. A. Dilhas, O. Ouerfelli, H. Zhao, and G. Yang are coinventors of an ARN-509 synthetic method. C.L. Sawyers and M.E. Jung are consultants to Aragon. C.L. Sawyers, M.E. Jung, J. Joseph, K. Grillot, E.D. Bischoff, A. Aparicio, G. Shao, J. Qian, J. Sensintaffar, M.R. Herbert, C. Bonnefous, B. Darimont, N.D. Smith, P.J. Rix, R.A. Heyman, J.H. Hager, and N.J. Clegg own Aragon stock. No potential conflicts of interest were disclosed by the other authors.

Acknowledgments

The authors thank S.P. Balk (Beth Israel Deaconess Medical Center) and M. Diamond (Washington University School of Medicine) for plasmids, P.A. Watson and Sawyers laboratory members for helpful discussions; F.M. Sirotnak, L.J. McDonald, and S. Sequira for operational guidance; and Q. Weige, C. Wa (Analytical Pharmacology); G. Sukenick, H. Liu, S. Ruesli, H. Fang (NMR Analytical Core); S. Monette, S.S. Couto, N. Pinard, J. Candelier, M. Jiao (Laboratory of Comparative Pathology); Molecular Cytology; Small-Animal Imaging Core Facility; S. Cai, E. Burnazi (Radiochemistry Core); and A.E. Lash (Bioinformatics) for MSKCC technical support.

Grant Support

This study was supported by Charles H. Revson Senior Fellowship in Life Sciences (to N.J. Clegg); ASCO Young Investigator Award, AACR BMS Fellowship, K08CA140946, DOD W81XWH-10-1-0197 (to Y. Chen); Department of Defense PCRP Prostate Cancer Training Award (to L. Cai); Howard Hughes Medical Institute, National Cancer Institute (5P01CA089021; to C.L. Sawyers); and NCI Core Grant (2 P30 CA 008748-43) for partial support of the Organic Synthesis Core (to O. Ouerfelli).

The costs of publication of this article were defrayed in part by the payment of page charges. This article must therefore be hereby marked *advertisement* in accordance with 18 U.S.C. Section 1734 solely to indicate this fact.

Received December 5, 2011; accepted January 2, 2012; published OnlineFirst January 20, 2012.

References

1. Jemal A, Siegel R, Xu J, Ward E. Cancer statistics, 2010. CA Cancer J Clin 2010;60:277–300.
2. Scher HI, Sawyers CL. Biology of progressive, castration-resistant prostate cancer: directed therapies targeting the androgen-receptor signaling axis. J Clin Oncol 2005;23:8253–61.
3. Chen Y, Clegg NJ, Scher HI. Anti-androgens and androgen-depleting therapies in prostate cancer: new agents for an established target. Lancet Oncol 2009;10:981–91.
4. Reid AH, Attard G, Danila DC, Oommen NB, Olmos D, Fong PC, et al. Significant and sustained antitumor activity in post-docetaxel,

Published OnlineFirst January 20, 2012; DOI:10.1158/0008-5472.CAN-11-3948

castration-resistant prostate cancer with the CYP17 inhibitor abiraterone acetate. J Clin Oncol 2010;28:1489–95.
5. Danila DC, Morris MJ, de Bono JS, Ryan CJ, Denmeade SR, Smith MR, et al. Phase II multicenter study of abiraterone acetate plus prednisone therapy in patients with docetaxel-treated castration-resistant prostate cancer. J Clin Oncol 2010;28:1496–501.
6. Tran C, Ouk S, Clegg NJ, Chen Y, Watson PA, Arora V, et al. Development of a second-generation antiandrogen for treatment of advanced prostate cancer. Science 2009;324:787–90.
7. Scher HI, Beer TM, Higano CS, Anand A, Taplin ME, Efstathiou E, et al. Antitumour activity of MDV3100 in castration-resistant prostate cancer: a phase 1-2 study. Lancet 2010;375:1437–46.
8. de Bono JS, Logothetis CJ, Molina A, Fizazi K, North S, Chu L, et al. Abiraterone and increased survival in metastatic prostate cancer. N Engl J Med 2011;364:1995–2005.
9. Foster WR, Car BD, Shi H, Levesque PC, Obermeier MT, Gan J, et al. Drug safety is a barrier to the discovery and development of new androgen receptor antagonists. Prostate 2010;71:480–8.
10. Wang Q, Carroll JS, Brown M. Spatial and temporal recruitment of androgen receptor and its coactivators involves chromosomal looping and polymerase tracking. Mol Cell 2005;19:631–42.
11. Wang Q, Li W, Liu XS, Carroll JS, Janne OA, Keeton EK, et al. A hierarchical network of transcription factors governs androgen receptor-dependent prostate cancer growth. Mol Cell 2007;27:380–92.
12. Clegg NJ, Sawyers CL. New York: Memorial Sloan-Kettering Cancer Center; 2010. Available from: http://cbio.mskcc.org/Public/Sawyers_Clegg_ARN-509_2010/.
13. Chen CD, Welsbie DS, Tran C, Baek SH, Chen R, Vessella R, et al. Molecular determinants of resistance to antiandrogen therapy. Nat Med 2004;10:33–9.
14. Taplin ME, Balk SP. Androgen receptor: a key molecule in the progression of prostate cancer to hormone independence. J Cell Biochem 2004;91:483–90.
15. Shidaifat F, Gharaibeh M, Bani-Ismail Z. Effect of castration on extracellular matrix remodeling and angiogenesis of the prostate gland. Endocr J 2007;54:521–9.
16. Carver BS, Chapinski C, Wongvipat J, Hieronymus H, Chen Y, Chandarlapaty S, et al. Reciprocal feedback regulation of PI3K and androgen receptor signaling in PTEN-deficient prostate cancer. Cancer Cell 2011;19:575–86.